Global J. Environ. Sci. Manage. 8(3): 353-368, Summer 2022, Serial #31

Global Journal of Environmental Science and Management
(GJESM)

Homepage: https://www.gjesm.net/

ORIGINAL RESEARCH ARTICLE

Impact of tropical Cyclone Marcus on ocean subsurface and surface layers

A.F. Koropitan*, M.H.I. Khaldun, Y. Naulita

Department of Marine Science and Technology, Faculty of Fisheries and Marine Science, IPB University, Kampus IPB Dramaga, Bogor 16680, Indonesia

ARTICLE INFO

Article History:
Received 02 September 2021
Revised 29 November 2021
Accepted 20 December 2021

Keywords:
Chlorophyll-a
Cyclone Marcus
Ocean temperature
Southeast Indian Ocean
Subsurface and surface layers
Eddy

ABSTRACT

BACKGROUND AND OBJECTIVES: The southeast Indian Ocean is one of the areas where tropical cyclones formed. A comprehensive understanding of the cyclone impact in the Southeastern Indian Ocean is needed to anticipate future changes due to the warming trend. The present study investigates the influence of Cyclone Marcus on oceanographic processes in the subsurface and surface layers and its impact on temperature and Chlorophyll-a in the Southeastern Indian Ocean. The present study applies the Argo Float data located near the peak of the Cyclone Markus path and could capture the subsurface layer vertically that has never been reported previously.
METHODS: This study performs Copernicus data set and Argo Float data to analyze the oceanographic feature of the region before, during, and after Cyclone Marcus.
FINDINGS: The average surface current velocity increased almost two times during Cyclone Marcus, and the eddy was formed in the clockwise direction following the surface wind pattern. The Argo Float data presents that Cyclone Marcus could induce surface divergence (clockwise eddy) where the cold water and high salinity waters pumped up to the surface layer, starting 1 day after the peak of Cyclone Marcus, resulting in cooling surface temperature by 1.7 °C and deepening mixed layer depth up to 60 m. It implies that the lifted nutrient-rich water stays in the mixed layer depth for 11 days, and sea surface Chlorophyll-a concentration increase with time lags of 2.5 days and 5.6 days, respectively. The Chlorophyll-a concentration increases 2.5 times, and since then starts to decrease its 'normal concentration' within two weeks.
CONCLUSION: Cyclone Marcus triggers the entrainment between the subsurface layer and the sea surface, forcing a phytoplankton growth, particularly in the path area. The future cyclone could increase in the category in the study area, as the warming trend in the Indian Ocean.

DOI: 10.22034/gjesm.2022.03.05

NUMBER OF REFERENCES	NUMBER OF FIGURES	NUMBER OF TABLES
35	9	2

*Corresponding Author:
Email: *alan@apps.ipb.ac.id*
Phone: +62 251 8623644
ORCID: 0000-0001-5794-094X

Note: Discussion period for this manuscript open until October 1, 2022 on GJESM website at the "Show Article".

INTRODUCTION

The Southeast Indian Ocean is one of the areas where tropical cyclones (TCs) formed. Generally, tropical cyclone seeds form in the Arafura Sea and the waters of Northern Australia, which continue to move southwest (Hoque *et al.*, 2017). The intensity of TCs will continue to move increasingly until their energy becomes extinct. The increase in cyclone intensity is forced by ocean temperature, where the relatively warm waters in the surface ocean could be a source of energy for TCs to maintain their existence (Pillay and Fitchett, 2021). The trend of the Indian Ocean warming, as reported by Roxy *et al.* (2015), is expected to affect the number and intensity of TCs. The temperature increase in a tropical ocean area could provide a low-pressure centre or a tropical depression that becomes the seed of TCs. A comprehensive understanding of the TCs impact in the Southeastern Indian Ocean is needed to anticipate future changes due to the warming trend. The negative impact of TCs, such as extreme weather, could cause material losses and casualties in the impacted coastal areas. Another encouraging impact was reported by Yu *et al.* (2013) that after the TCs Goni and Koppu, there was an increase in the abundance of fish offshore for up to eight days in the South China Sea. Yu *et al.* (2014) showed that TCs Chanthu, Vicente, and Kai-tak could increase catch per unit effort (CPUE) for up to three weeks in the Northwest of the South China Sea. The increased CPUE is closely related to the increase in Chlorophyll-a (Chl-a) after TCs. A similar thing could happen in the Southeastern Indian Ocean. Previous studies suggested a decrease in temperature and an increase in primary productivity triggered by TCs. Lü *et al.* (2020) reported that the phenomenon was due to the vertical entrainment that pumped up the relatively cold and nutrient-rich waters from the subsurface to surface layers. TCs will form eddies in the surface ocean along the cyclone path. The pressure difference in the surface ocean due to the lower centre of the cyclone will be filled by a water mass from the subsurface to surface layers (upwelling). The upwelling implied ocean fertility. Chacko and Zimik (2018) revealed that TCs could affect a surface mixed layer down to 100 m depth. The biological responses in the surface ocean can be different along the cyclone path, depending on the upwelling magnitude and the availability of nutrients in the water. The increase in primary productivity caused by TCs is temporary. After some time, primary productivity will decrease again at different intervals (Lü *et al.*, 2020). Comprehensive studies on the impact of TCs on ocean dynamics in the subsurface layer have been elaborated. The response of the water column in the subsurface was shown in the form of increasing mixed layer depth (MLD), which becomes deeper due to the turbulent mixing. Cyclone Phailin in the Bay of Bengal caused a MLD of 29 m (Vidya *et al.*, 2017). Cyclone Trami in the northwest Pacific Ocean showed a mixed layer change by 94 m (Chai *et al.*, 2021). A review paper by (Zhang, *et al.*, 2021) highlighted that the upper ocean response usually recovers in several days to several weeks, depending on the intensity, translation speed and size of the TCs. Environmental parameters are also important, such as ocean stratification and eddies. The ocean dynamics in the subsurface layer of the Southeast Indian Ocean influenced by TCs still need to be studied further. Most of the previous studies only report the oceanographic processes in the surface, as presented in Tabel 1.

The impact of TCs is quite significant on the surface and subsurface layers. What are the oceanographic characteristics in subsurface and surface layers of the Southeast Indian Ocean during and after TCs? The mechanism and impact on oceanographic processes in the subsurface layer that affect Chl-a and temperature in the surface layer of the Southeast Indian Ocean have not been studied previously. The present study aims to investigate in detail the influence of Cyclone Marcus on oceanographic processes in the subsurface and surface layers and its impact on SST and surface Chl-a in the Southeastern Indian Ocean in 2018. The present study applies the Argo Float data, which has stations simultaneously near the peak of the Cyclone Markus path. The Argo Float data could capture the oceanographic processes in the subsurface layer vertically that has never been reported previously in the Southeastern Indian Ocean.

MATERIALS AND METHODS

Description of the study area and data collection

Tropical Cyclone Marcus was an intense tropical cyclone in 2018 with a category 5 *Saffir-Simpson* scale where the TCs data were collected from the Australian Bureau of Meteorology (BOM). Cyclone Marcus seedlings formed in northern Australian

waters on 14 March 2018 and became extinct on 24 March 2018. Information and images of the trajectory of Cyclone Marcus are shown in Fig. 1. This study used oceanographic data set or derivative works from Copernicus Marine Service Information. The SST data are adopted from the Operational Sea Surface Temperature and Sea Ice Analysis (OSTIA) data. OSTIA uses satellite data provided by Group for High-Resolution Sea Surface Temperature (GHRSST) using field observations and satellite data that uses infrared and microwaves to determine the SST data. The use of microwaves can overcome the effects of

Table 1: Previous studies in the Southeastern Indian Ocean

No.	Tropical cyclones and references	Period	Category (*Saffir-Simpson* scale)	Data Set	Findings (highlighted in the abstract)
1	Ernie (Efendi *et al.*, 2018)	6-10 April 2017	4	Sea Surface Temperature (SST) and	SST decrease and Chl-a increase after the cyclone.
2	Seroja (Avrionesti *et al.*, 2021)	4-12 April 2021	2	SST (satellite data), Chl-a, MLD and sea surface height (E.U. Copernicus Marine Service Information), sea surface wind (satellite data).	SST decrease, Chl-a increase, sea surface height anomaly decrease, and MLD increase after the cyclone.
3	Seroja (Setiawan *et al.*, 2021)	4-12 April 2021	2	SST and Chl-a (satellite), sea surface wind (Cross-Calibrated Multi-Platform).	SST decrease and Chl-a increase after the cyclone.
4	Cempaka (Aditya *et al.*, 2021)	25-27 November 2017	1	SST and Chl-a (satellite), sea surface wind (Cross-Calibrated Multi-Platform).	SST decrease and Chl-a increase after the cyclone.
5	Dahlia (Aditya *et al.*, 2021)	27 November to 2 December	2	SST and Chl-a (satellite), sea surface wind (Cross-Calibrated Multi-	SST decrease and Chl-a increase after the cyclone.

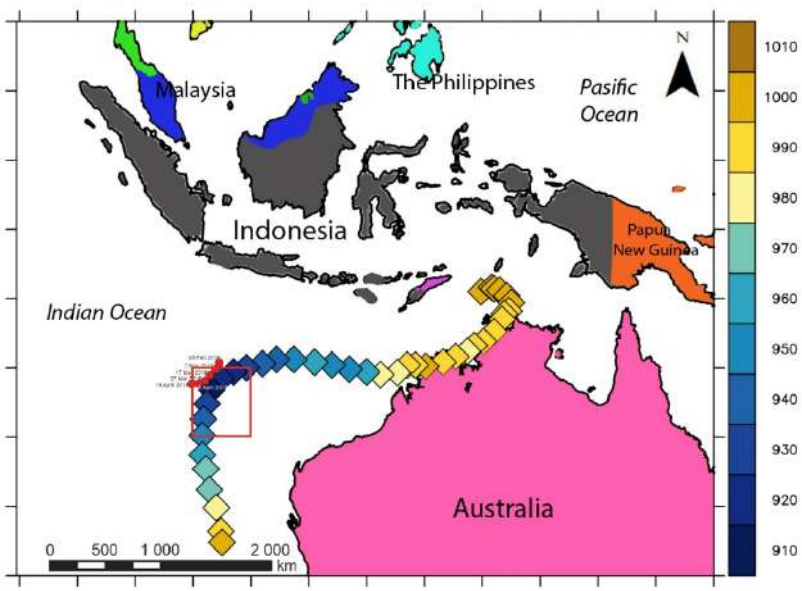

Fig 1: Path of Cyclone Marcus during 14-24 March 2018 and pressure (color in hPa), while the red dots indicate the position of Argo Float stations. The red box shows the study area indicating the highest intensity (low-pressure area) of Cyclone Marcus

clouds that form during TCs. SST data have a spatial resolution of 0.05° by 0.05° and daily temporal resolution (Donlon *et al.,* 2012). MLD data were obtained from a 3 dimension multi-observations product of the ocean (ARMOR3D) with a spatial resolution of 0.25° by 0.25° and a weekly temporal resolution (Guinehut *et al.,* 2012; Mulet *et al.,* 2012). Surface wind data has a spatial resolution of 0.25° by 0.25° and a temporal resolution of six hours, while ocean current data has a spatial resolution of 0.25° by 0.25° and a daily temporal resolution (Rio *et al.,* 2014). The Chl-a concentration data are based on the merging of the sensors Sea-viewing Wide Field-of-view Sensor (SeaWiFS), Moderate Resolution Imaging Spectroradiometer (MODIS), Medium Resolution Imaging Spectrometer (MERIS), The Visible and Infrared Imager/Radiometer Suite (VIIRS), the Suomi National Polar-orbiting Partnership (S-NPP), The Joint Polar Satellite System (JPSS), and Ocean and Land Color Instrument (OLCI) sensor. The Chl-a concentration data has a spatial resolution of 4 km by 4 km and a daily temporal resolution. Subsurface observations were examined using the Argo Float Commonwealth Scientific and Industrial Research Organization (CSIRO) Australia. The Argo Float is operational with a thermistor, conductivity sensor, and pressure gauge to record temperature, salinity, and depth, respectively, every ten days in the Southeastern Indian Ocean. The Argo Float data was chosen because of its location (17 March 2018 at 107.08°E and 15.68°S; 27 March 2018 at 106.72°E 15.92°S), which was on the path of Cyclone Marcus when it reached its lowest pressure peak so that it can provide information before and after the cyclone passes that location at 21-24 March 2018.

Data analysis

Spatial analysis is divided into three phases, namely before Cyclone Marcus (11-17 March 2018), during Cyclone Marcus (18-25 March 2018), and after Cyclone Marcus (26-31 March 2018). Spatial analysis is the average of each phase on each variable, using in Eq. 1.

$$\overline{x} = \frac{\sum_{i=1}^{n} x_i}{n} \quad (1)$$

where $\overline{x}$ is the average value of each phase, x_i is the sample's value, and n is the amount of data.

Accumulated Cyclone Energy (ACE) is a method to measure or quantify tropical cyclone phenomena based on the strength and timing of TCs in a particular area or time (Collins, 2018). The ACE value is obtained from the estimated maximum wind speed during the life of a tropical cyclone with 6-hour intervals. As for the calculation of ACE, using Eq. 2.

$$ACE = 10^{-4} \sum v^2_{max} \quad (2)$$

where v_{max} is the maximum constant wind speed at 6-hour intervals (m/s). *Ekman* pumping velocity (EPV) forced by TCs was calculated using Eqs. 3 and 4 (Chacko and Zimik, 2018).

$$\text{wind stress } (\tau) = \rho_{air} C_d U^2 \quad (3)$$

$$EPV = Curl(\tau) / \rho_w xf \quad (4)$$

where ρ_{air} is the density of air (1.25 kg/m^3), C_d is wind drag coefficient (1.3 x 10^{-3}), which is a dimensionless quantity, U is the wind speed, ρ_w is the density of seawater (1025 kg/m^3), and f is the *Coriolis* parameter. A positive (negative) value indicates an upwelling (downwelling) event. The relationship between SST, Chl-a, and ACE was analyzed using a wavelet transformation, which is a *Morlet* wavelet (Grinsted *et al.*, 2004).

RESULTS AND DISCUSSION

Surface ocean response to Cyclone Marcus

The response of the layer above sea level is often determined by observing changes in wind speed and current speed. During the peak of Cyclone Marcus (Fig. 2a), the lowest pressure occurs in the eye, where surface wind speed reached 20 m/s in a clockwise direction due to the Coriolis effect. The average surface wind speed before the occurrence of Cyclone Marcus (11–17 March 2018) was around 4-6 m/s in the study area (Fig. 2b). The average surface wind speed during Cyclone Marcus (18–25 March 2018) was in the range of 11-18 m/s in the study area (Fig. 2c). Besides that, Cyclone Marcus began to re-curvature to the South. The surface winds will accelerate as the intensity of TCs increases (Zhang *et al.,* 2020). After the cyclone reached the extinction

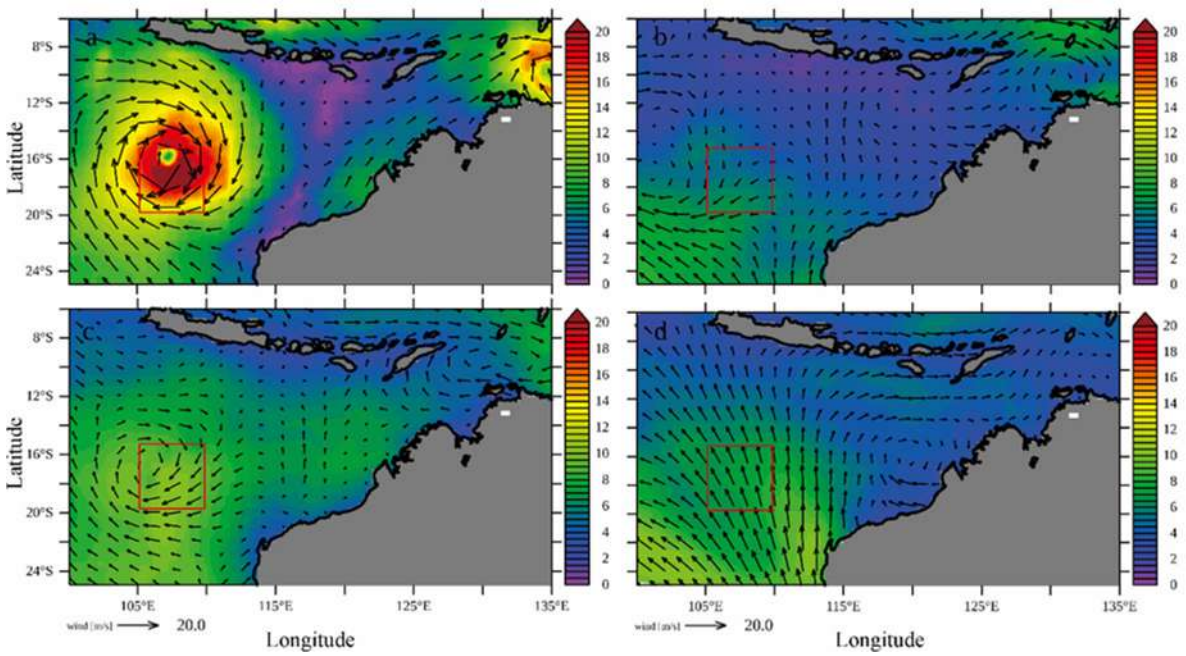

Fig. 2: The wind pattern (color in m/s): (a) during the peak of Cyclone Marcus on 22 March 2018, (b) before Cyclone Marcus (11-17 March 2018), (c) during Cyclone Marcus (18-25 March 2018), (d) after Cyclone Marcus (26-31 March 2018)

phase (26–31 March 2018), the average surface wind speed in the study area of Cyclone Marcus ranged 1-10 m/s (Fig. 2d). The surface wind speed decreased significantly, presumably because the post-tropical cyclone causes calmer weather with cold SST. SST cooling weakens the cyclone system because of no energy source (Sillmann *et al.,* 2021; Guo *et al.,* 2020).

Ocean flow patterns also show a significant response to Cyclone Marcus, particularly in the study area. During the peak of Cyclone Marcus (Fig. 3a), the eddy was formed in the clockwise direction following the surface wind pattern where surface current velocity reached 0.7 m/s. Before the cyclone, the average surface current velocity was around 0.19-0.23 m/s in the study area (Fig. 3b). The average surface current velocity during the occurrence of Cyclone Marcus ranged from 0.21-0.45 m/s in the study area (Fig. 3c), which is in line with the movement direction of the cyclone towards the South. The movement of surface currents changed significantly, while the currents increased as the cyclone intensity was high. The current velocity decreased close to normal after the cyclone, with its average value ranging at 0.2-0.23 m/s in the study area (Fig. 3d). The decrease in currents is not as significant as that in the wind since the currents are not directly related to TCs and only receive the influence of energy transfer from wind friction (Zhang *et al.,* 2020).

The response of temperature and salinity in the subsurface

Cyclone Marcus affects the sea surface layer and the subsurface layer as indicated by a response of physical and biological parameters (Chacko and Zimik, 2018). The present study performs the Argo Float data located near the trajectory of Cyclone Marcus that shows temporal changes in temperature and salinity below the surface, particularly at depths of 4 m to 100 m, as presented in Fig. 4. The water temperature in the surface layer before Cyclone Marcus showed a value of 28.53 °C, which continued to increase to 29.49 °C (Fig. 4a). Before the cyclone, the value of 27.79 °C at 30 m depth continued to increase by 28.91 °C during the cyclone, where the turbulent mixing and upwelled water from the subsurface to surface layers occurred. This mechanism subsequently decreased the temperature on the surface after the cyclone. Fig. 4a shows the temperature at 52 m depth

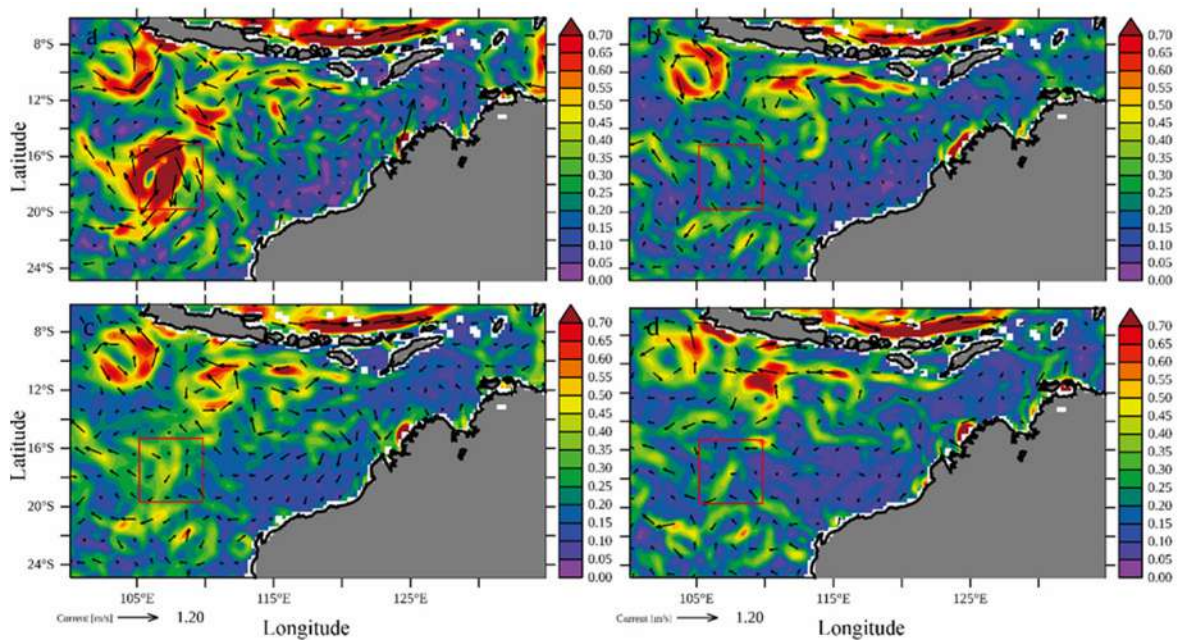

Fig. 3: The ocean flow pattern (color in m/s): (a) during the peak of Cyclone Marcus on 22 March 2018, (b) before Cyclone Marcus (March 11-17), (c) during Cyclone Marcus (March 18-25), (d) after Marcus (March 26-31)

reached 28.28 °C as the cyclone became extinct. The temperature at a depth layer of 4 – 52 m is relatively similar, indicating an increase in temperature. This response is due to temperature inversion below the surface. The temperature inversion causes an increase in the surface layer temperature. The temperature inversion significantly increases the temperature in the subsurface before the cyclone and later increases SST (Chacko and Zimik, 2018). Fig. 4b shows the salinity changes in the subsurface. Before the cyclone, salinity at a depth layer of 0-22m showed a low salinity <34.25 PSU. During the cyclone, the vertical mixing caused a significant increase in salinity, reaching 34.668 PSU at 46 m depth. After the cyclone was extinct, it took time to return to normal, which varies from a few days to a few weeks (Chacko and Zimik, 2018; Yan *et al.,* 2017). Fig. 4b clearly shows an upwelling event during the cyclone, which ended ten days after the cyclone. The occurrence of upwelling is the consequence of the clockwise eddy that triggers surface divergence. Turbulent mixing also changes MLD in the study area, where the MLD before the cyclone was counted around 22 – 26 m depths (Fig. 5a). During the cyclone, MLD ranged between 20 until 25 m depths (Fig. 5b). After the cyclone, MLD has seen around 18 – 40 m depths (Fig. 5c). In comparison with Fig. 4a, a MLD before the cyclone of 30 m depth and after the cyclone of 60 m depth. The MLD in Fig. 5 was adopted from ARMOR3D (Copernicus data set), while the MLD in Fig. 4a was an estimation from the vertical temperature profile of the Argo Float Data.

Sea surface temperature response

The SST response to TCs is clearly illustrated by the relatively low SST values, where the spatially averaged SST in the study area was 28.04 °C before Cyclone Marcus (Fig. 6a) and decreased to around 27.5 °C during Cyclone Marcus (Fig. 6b). Table 2 presents the comparison of SST as reported in the previous studies. This mechanism is presumably due to the influence of water mass mixing, upwelling, and heat release. About 85% of the causes of SST cooling due to TCs are caused by upwelling or entrainment processes, in addition to the heat release process used by TCs as energy to maintain their existence (Sillmann *et al.,* 2021). The initially warm SST value will be the heat intake used by the cyclone as an energy source to maintain its existence for more prolonged movements. Each tropical cyclone has a different SST threshold value, and the threshold depends on

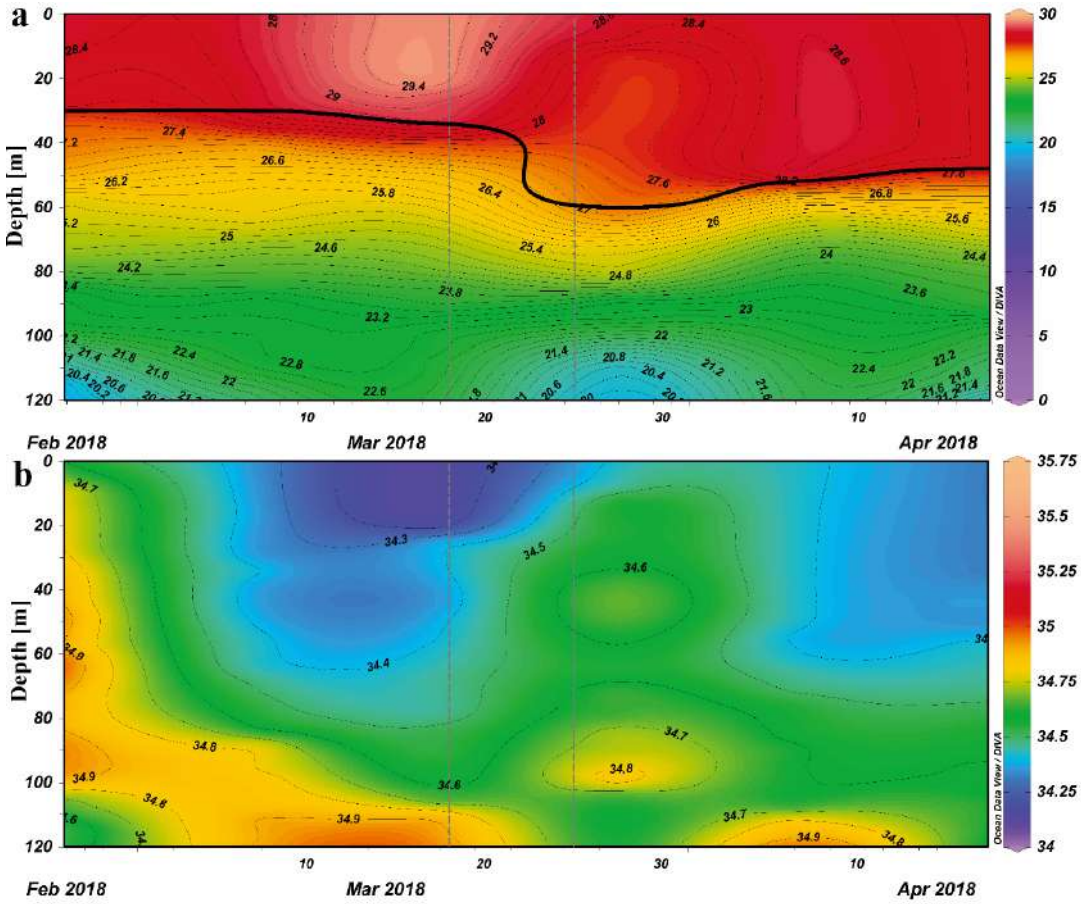

Fig. 4: Vertical profile of temperature (color in °C) (a), and salinity (color in PSU) (b) at Argo Float stations. The thick contour-line in (a) indicates a MLD. A thick vertical dash-line indicates the occurrence of Cyclone Marcus between 18 and 25 March 2018. Data interpolation among the Argo Float stations and visualization was carried out using Ocean Data View with DIVA (Data Interpolating Variational Analysis) method (Schlitzer, 2021)

the lifetime of the cyclone (Tory and Dare., 2015) so that each tropical cyclone has an SST value that varies in experiencing intensification (increase in energy), de-intensification (decrease in energy), re-curvature, and even dissipation (Chacko and Zimik, 2018). The spatially averaged SST value after Cyclone Marcus in the study area was around 27.11 °C (Fig. 6c). The dissipation stage started after the cyclone, as seen by slowly increased SST until 27.34 °C. That means the ocean response was indicated to restore SST to an original or stable condition. During pre-and post- Cyclone Marcus, the SST difference reached 1.7 °C. The magnitude of SST difference caused by the cyclone is strongly influenced by its intensity which causes vertical mixing in the surface ocean. The SST variability can determine the intensity of TCs (Xu *et al.,* 2016; Thanh *et al.,* 2019).

Biological response

The spatial and temporal response of Chl-a in the sea surface affected by Cyclone Marcus showed an increased concentration along the cyclone path. The present study focuses on the Chl-a response in the area where the peak intensity (category 5) occurred. The Chl-a concentration before Cyclone Marcus was around 0.065-0.081 mg/m^3 in the study area (Fig. 7a). The present results correspond with previous research conducted by Li *et al.* (2012) regarding the vertical distribution of Chl-a in the Indian Ocean, which shows the concentration of Chl-a in the surface layer in the East Indian Ocean is less than 0.10 µg/L (equal to mg/m^3). The concentration of Chl-a during

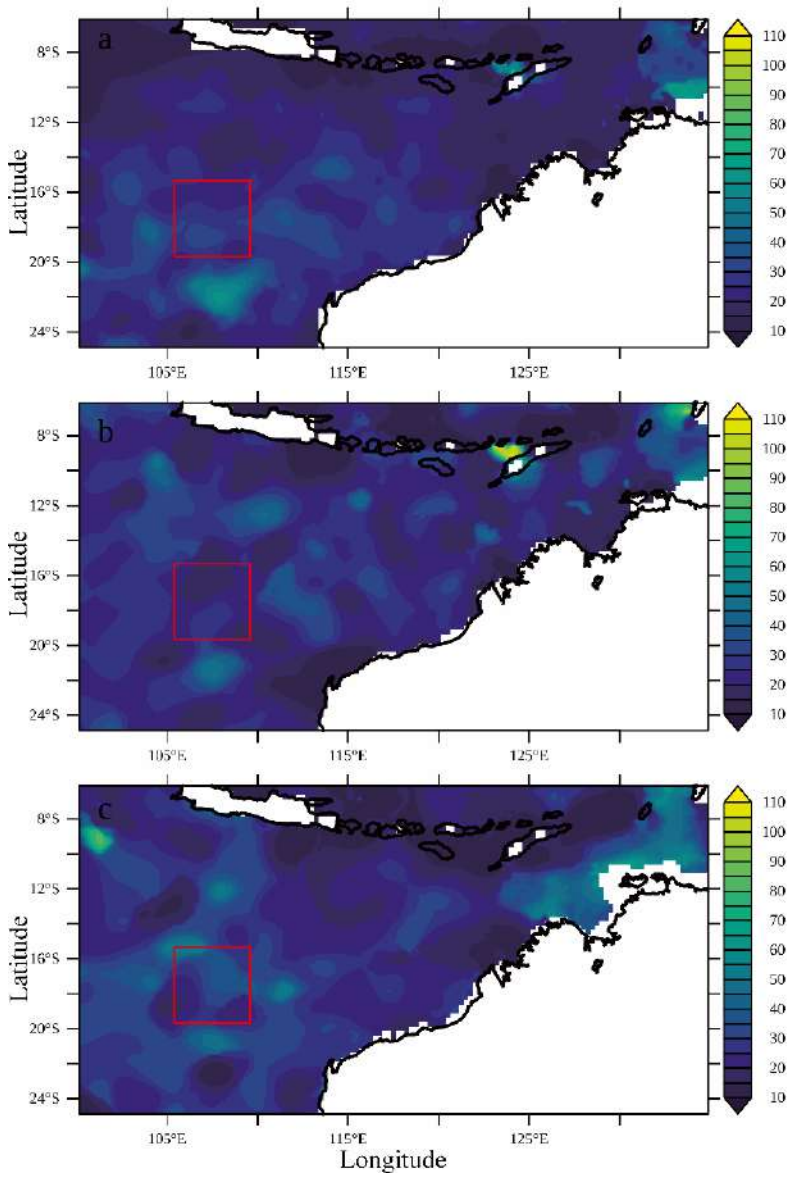

Fig. 5: Distribution of weekly MLD (color in m): (a) before Cyclone Marcus (11-17 March 2018), (b) during Cyclone Marcus (18-25 March 2018), (c) after Cyclone Marcus (26-31 March 2018)

Cyclone Marcus showed an increase of 0.072- 0.14 mg/m^3 in the study area (Fig. 7b) and continued to increase after the cyclone with a range of 0.114- 0.186 mg/m^3 in the study area (Fig. 7c). As for comparison, the Chl-a concentrations from the previous studies are shown in Table 2. The response of Chl-a showed the most significant increase in concentration on 27 March 2018, which reached 0.186 mg/m^3 or 2.5 times greater than the average concentration of 0.075 mg/m^3 before the cyclone. The present study confirms a time lag of the Chl-a response during the occurrence of Cyclone Marcus and the nutrient enrichment process around the cyclone path.

Several factors might influence the process of increasing Chl-a in the sea surface layer. The present study highlights that wind-induced EPV plays a

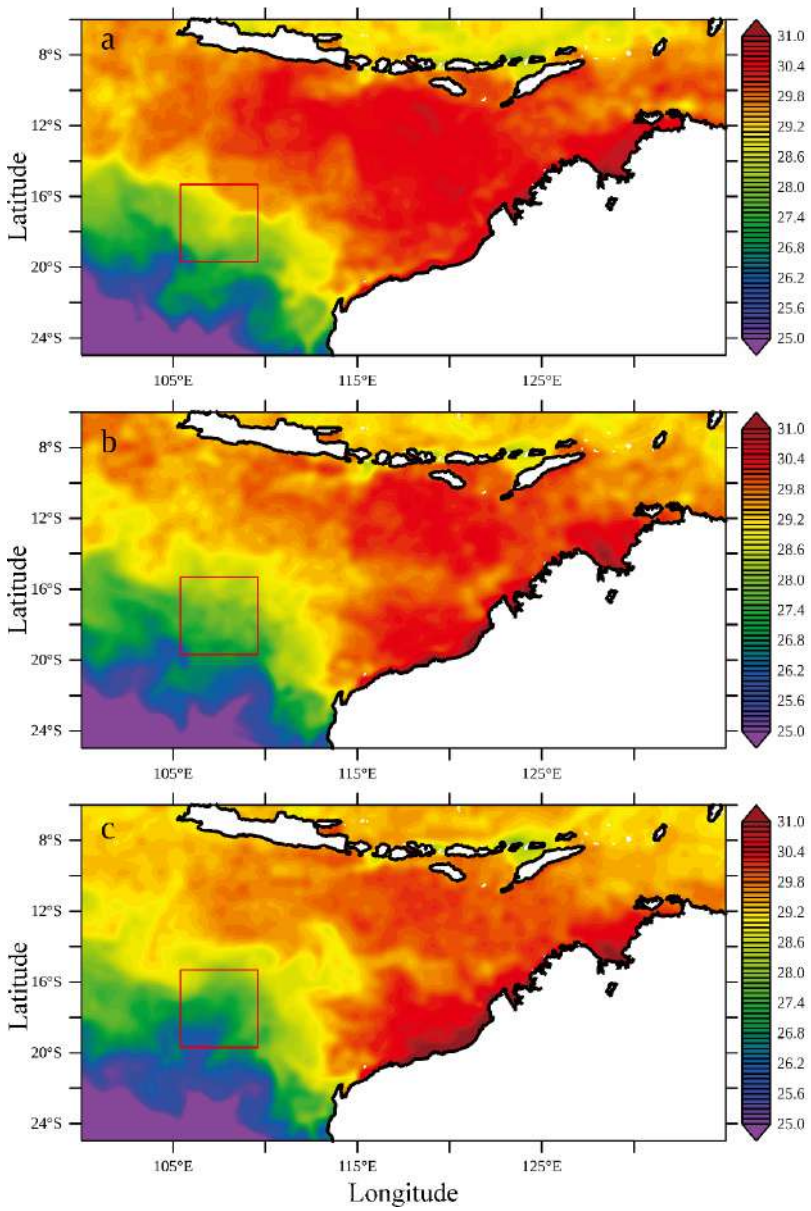

Fig. 6: Distribution of SST (color in °C): (a) before Marcus (11-17 March 2018), (b) during Marcus 18-25 March 2018), (c) after Marcus (26-31 March 2018)

significant role in determining the upwelling. The wind generated by Cyclone Marcus produces a positive (negative) value, indicating an upwelling (downwelling) event, as shown in Fig. 8. The increase in Chl-a concentration is consequently affected by the upwelling process that causes a nutrient-rich water mass to pump up to the surface (Chacko and Zimik, 2018; Efendi *et al.*, 2018). As discussed previously, Cyclone Marcus can mix up 60 m depth. Li *et al.* (2012) reported that the Depth Chl-a Maximum (DCM) was at 55.6 m to 91 m depths in the East Indian Ocean. The nutrients and Chl-a concentrations in DCM were carried to the surface and increased the concentration of Chl-a. The increase in Chl-a after the cyclone was

Table 2: SST and sea surface Chl-a of the previous studies in the Southeastern Indian Ocean

No.	TCs and references	Period	Category (*Saffir-Simpson* scale)	SST (°C)		Chl-a (mg/m^3)	
				Before TCs	After TCs	Before TCs	After TCs
1	Ernie (Efendi *et al.*, 2018)	6-10 April 2017	4	30 - 32	24 -27	0.08	0.15
2	Seroja (Avrionesti *et al.*, 2021)	4-12 April 2021	2	29.72	26.32	Not available	2.57
3	Seroja (Setiawan *et al.*, 2021)	4-12 April 2021	2	29.8	<28	Not available	>12
4	Cempaka (Aditya *et al.*, 2021)	25-27 November 2017	1	29.3	28.2	0 - 0.12	0.15 - 0.2
5	Dahlia (Aditya *et al.*, 2021)	27 November - 2 December 2017	2	28 - 32	26 - 27	0 - 0.12	0.2 - 0.35

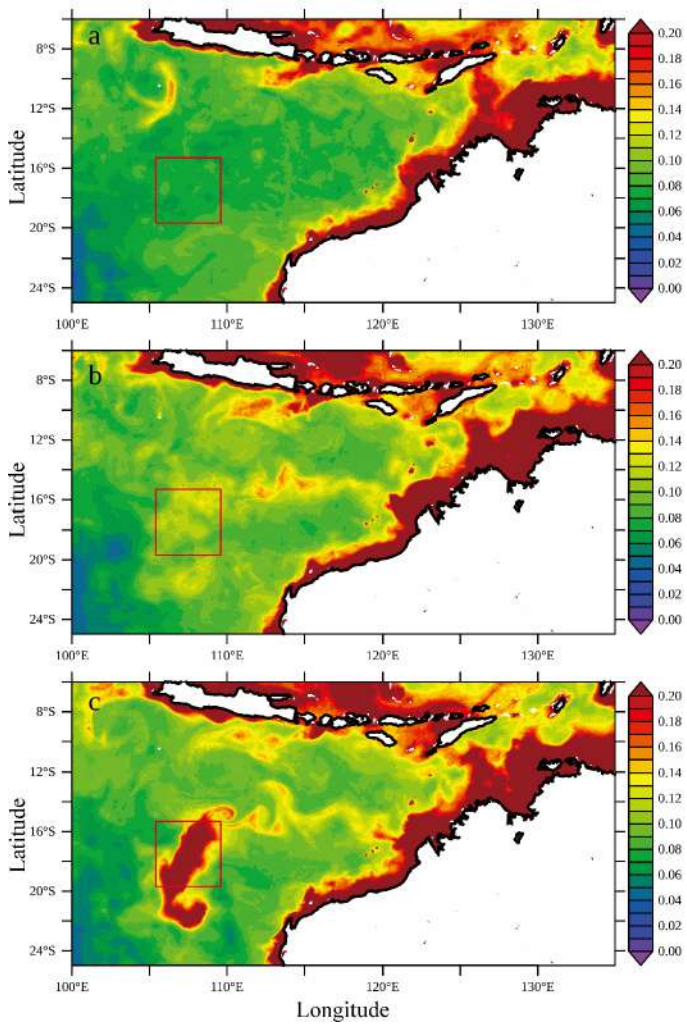

Fig. 7: Distribution of sea surface Chl-a (color in mg/m^3): (a) before Cyclone Marcus (11-17 March 2018), (b) during Cyclone Marcus (18-25 March 2018), (c) after Cyclone Marcus (26-31 March 2018)

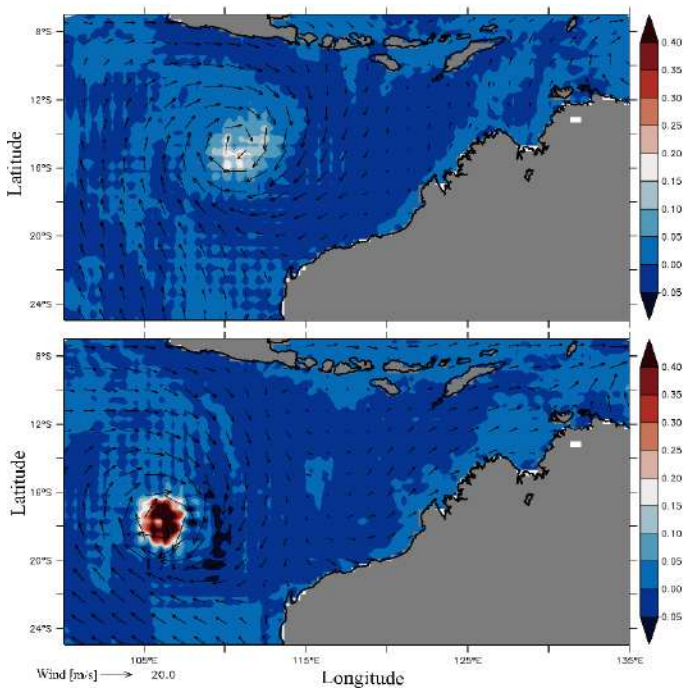

Fig. 8: Distribution of EPV [color in x10^{-5} m/s] during: (a) Cyclone Marcus category 4 (21 March 2018), (b) Cyclone Marcus category 5 (22 March 2018)

due to the shallowing MLD and thermocline depth, which subsequently provided nutrient enrichment in the surface layer (Chakraborty *et al.,* 2018). After 27 March 2018, the Chl-a concentration continued to decrease until its concentration reached the monthly average without the cyclone effects on 10 April 2018. The present finding presents that Cyclone Marcus could induce surface divergence (clockwise eddy) where the cold water and high salinity waters pumped up to the surface layer, starting from 23 March (1 day after the peak of Cyclone Marcus) to 4 April 2018 (Fig. 4). It implies that the lifted nutrient-rich water stays in the MLD for 11 days, and a Chl-a increases two weeks after the cyclone. A similar phenomenon was also found by Lü *et al.* (2020), with the Chl-a concentration increase persisting for up to ten days, while Mandal *et al.* (2018) found up to eight days. Chakraborty *et al.* (2018) and Efendi *et al.* (2018) reported that the Chl-a concentration increase could last two to three weeks after a storm. As affected SST, the speed and intensity of the cyclone affect the vertical mixing and upwelling processes (Fig. 8a and Fig. 8b). The present study found that category four or intensity four of the cyclone resulted in EPV value around 2.6 x 10^{-6} m/s, while in category five, the EPV value increased significantly by 3.01 x 10^{-4} m/s. The speed and intensity of the cyclone will subsequently increase the concentration of nutrients and trigger the growth of phytoplankton and increase the Chl-a concentration (Chacko and Zimik, 2018; Lin, 2012; Mei *et al.,* 2015).

Relationship between SST, Chl-a, and ACE

The response of SST and sea surface Chl-a concentration during the formation of TCs showed a strong relationship around the path of TCs. Our findings showed that the SST decreased and the Chl-a concentration increased along the cyclone path. Increasing (decreasing) Chl-a concentration (SST) depended on the intensity of TCs caused by the wind speed that forced mixing in the surface layer. The wavelet transforms cross-correlation between SST, Chl-a, and ACE (represents wind speed) in the study area during 2017-2018, as shown in Fig. 9. The present study found an increasing value of the wavelet spectrum from the end of March 2018 to the beginning of April 2018 with ten days. The phase relationship between variables is indicated by the

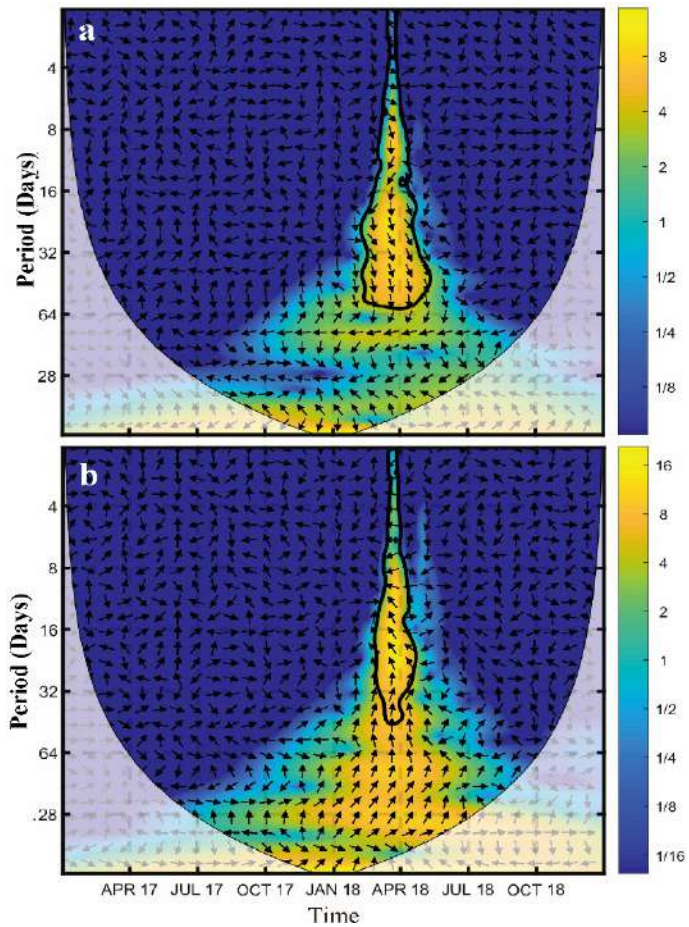

Fig. 9: Wavelet cross transformations in the study area where the thick black contours show a 95% confidence level for: (a) ACE and SST, (b) ACE and Chl-a. The wavelet calculation and visualization were carried out using MatLab R2020b

direction of the arrow in the wavelet analysis, where the arrow indicates the in-phase (anti-phase) to the right (left). The direction of the arrow starts from the right arrow to represent a time lag between the two variables. In this case, the arrows pointing to the lower right or upper left indicate the variable-1 (ACE) occurs first, while the arrows pointing to the upper right or lower left indicate that the variable-2 (SST and Chl-a) occurs first (Fig. 9). The time lag between the peak of Cyclone Marcus and the SST decrease was about 2.5 days (Fig. 9a). The coherence value for SST during the cyclone is 0.8, indicating that the two variables have a strong relationship. The present study also found that the time lag corresponds with the *Ekman* pumping response of 2.3 days, where the maximum EPV shows a value of 3.01 x 10^{-4} m/s consistent with the highest intensity in the study area. The water-mass entrainment from the lowest depth of MLD, which is 60 m, to the sea surface requires 2.3 days. The time lag between the peak of Cyclone Marcus and the Chl-a concentration increase was about 5.6 days (Fig. 9b). The coherence value for Chl-a during the cyclone shows a strong relationship among the two variables, which is 0.8. The present findings suggest that the mixing process due to upwelling would produce a different time lag for SST and Chl-a responses according to the wavelet analysis. In this case, the SST response is shorter than Chl-a because of the direct response of this SST parameter in the sea surface. It is different for the Chl-a parameter that needs a pre-response for nutrient enrichment in the surface from the subsurface layer before a

photosynthesize process for phytoplankton growth (Chl-a increase). Kämpf and Chapman (2016) stated that the movement of water masses from the water column takes several days to a week, which is sufficient time to lift the water mass to a vertical distance of 100 m or more. The difference in TCs intensity may cause a different time lag for the Chl-a response (Parker *et al.,* 2017). The Chl-a response relates to the pyramidal structure of the ecosystem in the upwelling regions, where primary, secondary and small pelagic fish productivities have a different time for their growths.

CONCLUSION

Cyclone Marcus in 2018 was one of TCs with high intensity of category 5 in the Southeastern Indian Ocean. The present study investigates the influence of Cyclone Marcus on oceanographic processes in the subsurface and surface layers and its impact on SST and surface Chl-a in the study area. The average surface wind speed increased by three times during Cyclone Marcus in a clockwise direction and decreased significantly after the cyclone reached the extinction phase due to SST cooling in the study area, resulting in no energy source for the cyclone. The average surface current velocity increased almost two times during Cyclone Marcus, and the eddy was formed in the clockwise direction following the surface wind pattern. The decrease in post-cyclone currents was not as drastic as the wind because the ocean friction limited energy transfer from the wind. The Argo Float data presents that Cyclone Marcus could induce surface divergence (clockwise eddy) where the cold water and high salinity waters pumped up to the surface layer, starting 1 day after the peak of Cyclone Marcus. It implies that the lifted nutrient-rich water stays in the MLD for 11 days, and a Chl-a increases two weeks after the cyclone. Wind-induced eddy and EPV play a significant role in determining the upwelling. Cyclone Marcus can mix up 60 m depth where the nutrients and Chl-a concentrations in DCM were carried to the surface and increased the concentration of Chl-a. The increase in Chl-a after the cyclone was due to the shallowing MLD and thermocline depth, which subsequently provided nutrient enrichment in the surface layer. Significant findings in this research show a SST difference of 1.7 °C, MLD deepening up to 60 m, and an increase in Chl-a almost three times in responding to the cyclone. The future TCs could increase in the category in the study area, as the warming trend in the Indian Ocean. Besides its negative impacts, future research could focus on the marine food chain as the phytoplankton blooming (Chl-a) after the cyclone.

AUTHOR CONTRIBUTIONS

A.F. Koropitan performed the literature review, research design, analyzed and interpreted the data, prepared the manuscript text and manuscript edition. M.H.I. Khaldun performed the literature review, data analysis and visualization, and manuscript preparation. Y. Naulita enriched the literature review and manuscript preparation.

ACKNOWLEDGEMENT

The authors wish to acknowledge the use of the PyFerret and Ocean Data View softwares for analysis and graphics in this paper. *PyFerret* is a product of NOAA's Pacific Marine Environmental Laboratory. The authors are grateful to Randi Firdauss for helping us in wavelet analysis using MatLab. This study has been conducted at Big Data and Ocean Modeling (BiOM) Laboratory, Department of Marine Science and Technology, IPB University.

CONFLICT OF INTEREST

The author declares that there is no conflict of interests regarding the publication of this manuscript. In addition, the ethical issues, including plagiarism, informed consent, misconduct, data fabrication and/or falsification, double publication and/or submission, and redundancy have been completely observed by the authors.

PUBLISHER'S NOTE

GJESM Publisher remains neutral with regard to jurisdictional claims in published maps and institutional affiliations.

ABBREVIATIONS

%	Percent
<	Less than
°	Degree
°C	Degree celsius
°E	Degree east
°S	Degree south
τ	Wind stress
µg/L	Microgram per liter
ACE	Accumulated cyclone energy
ARMOR3D	A 3 dimension multi-observations product of the ocean
BiOM	Big data and ocean modeling
BOM	Bureau of meteorology
C_d	Wind drag coefficient
Chl-a	Chlorophyll-a
CPUE	Catch per unit effort
CSIRO	Commonwealth scientific and industrial research organization
DCM	Depth chlorophyll maximum
DIVA	Data interpolating variational analysis
EPV	*Ekman* pumping velocity
Eq	Equation
	Coriolis parameter
Fig	Figure
GHRSST	Group for high-resolution sea surface temperature
hPa	Hectopascal
JPSS	Joint polar satellite system
kg/m³	Kilogram per cubic meter
Km	Kilometers
m	Meter
m/s	Meter per second
MERIS	Medium resolution imaging spectrometer
mg/m³	Milligram per cubic meter
MLD	Mixed layer depth
MODIS	Moderate resolution imaging spectroradiometer
n	Amount of data
OLCI	Ocean and land color instrument
OSTIA	The operational sea surface temperature and sea ice analysis
ρ_{air}	Density of air
ρ_w	Density of seawater
PSU	Practical salinity unit
S-NPP	Suomi national polar-orbiting partnership
SeaWiFS	Sea-viewing wide field-of-view sensor
SST	Sea surface temperature
TCs	Tropical cyclones
U	Wind speed
v	Maximum constant wind speed
VIIRS	Visible and infrared imager/radiometer suite
v_{max}	Maximum constant wind speed at 6-hour intervals
$\bar{x}$	Average value of each phase
xi	Sample's value

REFERENCES

Aditya, H.N.; Wirasatriya, A.; Kunarso.; Ismunarti, D.H.; Yusuf, M.; Rifai, A.; Purwanto.; Ismanto, A.; Widiaratih, R., (2021). Impact of tropical cyclones Cempaka and Dahlia to the variability of chlorophyll-a and sea surface temperature in the seas southern coast of Java Island. Ecol. Environ. Cnsev., 27: 379-387 **(9 pages).**

Avrionesti.; Khadami, F.; Purnaningtyas, D.W., (2021). Ocean response to tropical cyclone Seroja at East Nusa Tenggara waters. IOP Conference Series: Earth and Environmental Science, 925: 1-9 (**9 pages**).

Chacko, N.; Zimik, L., (2018). Effect of cyclone Thane in the Bay of

Bengal explored using moored buoy observations and multi-platform satellite data. J. Indian Soc. Remote Sens., 46: 821–828 (**8 pages**).

Chai, F.; Wang, Y.; Xing, X.; Yan, Y.; Xue, H.; Wells, M.; Boss, B., (2021). A limited effect of sub-tropical typhoons on phytoplankton dynamics. Biogeosciences. 18: 849–859 (**10 Pages**).

Chakraborty, K.; Nimit, K.; Akhand, A.; Prakash, S.; Paul, A.; Ghosh, J.; Udaya Bhaskar, T.V.S.; Chanda, A., (2018). Modeling the enhancement of sea surface chlorophyll concentration during the cyclonic events in the Arabian Sea. J. Sea Res., 140: 22–31 (**10 pages**).

Collins, D.J., (2018). Worldwide tropical cyclone activity measured using the actuaries climate index® methodology. Casualty Actuar. Soc. E-Forum., 2: 1 (**32 pages**).

Donlon, C.J.; Martin, M.; Stark, J.; Roberts-Jones, J.; Fiedler, E.; Wimmer, W., (2012). The Operational sea surface temperature and sea ice analysis (OSTIA) system. Remote Sens. Environ., 116: 140–158 (**19 pages**).

Efendi, U.; Fadlan, A.; Hidayat, A.M., (2018). Chlorophyll-a variability in the southern coast of Java Island, Indian Ocean: corresponding to the tropical cyclone of Ernie. IOP Conference Series: Earth and Environmental Science, 162: 1-12 (**12 pages**).

Grinsted, A.; Moore, J.; Jevrejeva S., (2004). Application of the cross wavelet transform and wavelet coherence to geophysical time series. Nonlinear Processes Geophys., 11(4): 561–566 (**6 pages**).

Guinehut, S.; Dhomps, A.L.; Larnicol, G.; Le Traon, P.Y., (2012). High resolution 3-d temperature and salinity fields derived from in situ and satellite observations. Ocean Sci., 8: 845–857 (**13 pages**).

Guo, T.; Sun, Y.; Liu, L.; Zhong, Z., (2020). The impact of storm-induced sst cooling on storm size and destructiveness: results from atmosphere–ocean coupled simulations. J. Meteorolog. Res., 34(5): 1068-1081 (**14 pages**).

Hoque, M.A.A.; Phinn, S.; Roelfsema, C., (2017). A systematic review of tropical cyclone disaster management research using remote sensing and spatial analysis. Ocean Coast. Manage., 146: 109–120 (**12 pages**).

Kämpf, J.; Chapman, P., (2016). Upwelling Systems of the World: A scientific journey to the most productive marine ecosystems. Switzerland, Swiss. Spinger International Publishing Switzerland.

Li, G.; Lin, Q.; Ni, G.; Shen, P.; Fan, Y.; Huang, L.; Tan, Y., (2012). Vertical patterns of early summer chlorophyll a concentration in the Indian Ocean with special reference to the variation of deep chlorophyll maximum. J. Mar. Biol., 2012: 1–6 (**6 pages**).

Lin, I.I., (2012). Typhoon-induced phytoplankton blooms and primary productivity increase in the western North Pacific subtropical ocean. J. Geophys. Res. C: Oceans., 117: 1-15 (**15 pages**).

Lü, H.; Zhao, X.; Sun, J.; Zha, G.; Xi, J.; Cai, S., (2020). A case study of a phytoplankton bloom triggered by a tropical cyclone and cyclonic eddies. PLoS One, 15: 1–18 (**18 pages**).

Mandal, S.; Sil, S.; Shee, A.; Venkatesan, R., (2018). Upper ocean and subsurface variability in the Bay of Bengal during cyclone ROANU: a synergistic view using in situ and satellite observations. Pure Appl. Geophys., 175: 4605–4624 (**20 pages**).

Mei, W.; Lien, C.C.; Lin, I.I.; Xie, S.P., (2015). Tropical cyclone-induced ocean response: a comparative study of the South China Sea and tropical Northwest Pacific. J. Clim., 28: 5952–5968 (**17 pages**).

Mulet, S.; Rio, M.H.; Mignot, A.; Guinehut, S.; Morrow, R., (2012). A new estimate of the global 3d geostrophic ocean circulation based on satellite data and in-situ measurements. Deep Sea Res. Part II., 77–80: 70-81 (**12 pages**).

Parker, C.; Lynch, A.; Spera, S.; Spangler, K., (2017). The relationship between tropical cyclone activity, nutrient loading, and algal blooms over the Great Barrier reef. Biogeosci. Discuss., 1–35 (**35 pages**).

Pillay, M.T.; Fitchett, M.T., (2021). On the conditions of formation of southern hemisphere tropical cyclones. Weather Clim. Extremes, 34(100376): 1-12 (**12 pages**).

Rio, M.H.; Mulet, S.; Picot, N., (2014). Beyond GOCE for the ocean circulation estimate: synergetic use of altimetry, gravimetry, and in situ data provides new insight into geostrophic and Ekman currents. Geophys. Res. Lett., 41: 8918–8925 (**8 pages**).

Roxy, M.K.; Ritika, K.; Terray, P.; Murtugudde, R.; Ashok, K.; Goswami, B.N., (2015). Drying of Indian subcontinent by rapid Indian Ocean warming and a weakening land-sea thermal gradient. Nat. Commun., 1-6 (**6 pages**).

Schlitzer, R., (2021). Ocean data view user 's guide.

Setiawan, R.Y.; Susanto, R.D.; Wirasatriya, A.; Alifdini, I.; Puryajati, A.D.; Maslukah, L.; Nurdin, N., (2021). Impacts of tropical cyclone Seroja on the phytoplankton chlorophyll-a and sea surface temperature in the Savu Sea, Indonesia. IEEE Access, 21: 152938-152944 (**7 pages**).

Sillmann, J.; Daloz, A.S.; Schaller, N.; Schwingshackl, C., (2021). Climate change 3rd ed: observed impacts on planet earth. United States. Elsevier Inc, USA.

Thanh, N. T.; Cuong, H. D.; Hien, N. X.; Kieu, C., (2019). Relationship between sea surface temperature and the maximum intensity of tropical cyclones affecting Vietnam's coastline. Int. J. Climatol., 40: 2527–2538 (**12 pages**).

Tory, K. J.; Dare, R. A., (2015). Sea surface temperature thresholds for tropical cyclone formation. J. Clim., 28(20): 8171–8183 (**13 pages**).

Vidya, P.J.; Das, S.; Murali.R, M., (2017). Contrasting chl-a responses to the tropical cyclones Thane and Phailin in the Bay of Bengal. J. Mar. Syst., 165: 103-114 (**12 pages**).

Xu, J.; Wang, Y.; Tan, Z., (2016). The relationship between sea surface temperature and maximum intensification rate of tropical cyclones in the North Atlantic. J. Atmos. Sci., 73: 4979-4988 (**10 pages**).

Yan, Y.; Li, L.; Wang, C., (2017). The effects of oceanic barrier layer on the upper ocean response to tropical cyclones. J. Geophys. Res. C: Oceans., 122: 4829–4844 (**16 pages**).

Yu, J.; Tang, D.; Chen, G.; Li, Y.; Huang, Z.; Wang, S., (2014). The positive effects of typhoons on the fish CPUE in the South China Sea. Cont. Shelf Res., 84: 1–12 (**12 pages**).

Yu, J.; Tang, D.; Li, Y.; Huang, Z.; Chen, G., (2013). Increase in fish abundance during two typhoons in the South China Sea. Adv. Space Res., 51: 1734–1749 (**16 pages**).

Zhang, H.; He, H.; Zhang, W.; Tian, D., (2021). Upper ocean response to tropical cyclones: a review. Geosci. Lett., 8(1): 1-12 (**12 pages**).

Zhang, H.; Liu, X.; Wu, R.; Chen, D.; Zhang, D.; Shang, X.; Wang, Y.; Song, X.; Jin W.; Yu, L.; Qi, Y.; Di Tian, D.; Zhang, W., (2020). Sea surface current response patterns to tropical cyclones. J. Mar. Syst., 208(103345): 1-16 (**16 pages**).

AUTHOR (S) BIOSKETCHES

Koropitan, A.F., Ph.D., Associate Professor, Department of Marine Science and Technology, Faculty of Fisheries and Marine Science, IPB University, Kampus IPB Dramaga, Bogor 16680, Indonesia.
- Email: *alan@apps.ipb.ac.id*
- ORCID: 0000-0001-5794-094X
- Web of Science ResearcherID: ABE-7099-2021
- Scopus Author ID: 23135214600
- Homepage: https://itk.ipb.ac.id/~itkipb/dr-alan-frendy-koropitan-s-pi-m-si/

Khaldun, M.H.I., M.Sc., Department of Marine Science and Technology, Faculty of Fisheries and Marine Science, IPB University, Kampus IPB Dramaga, Bogor 16680, Indonesia.
- Email: *mhikhaldun@gmail.com*
- ORCID: 0000-0003-2161-8136
- Web of Science ResearcherID: ABF-1690-2021
- Scopus Author ID: 57202966767
- Homepage:https://ipb.ac.id/faculty/index/faculty-of-fisheries-and-marine-science/department-of-marine-science-and-technology

Naulita, Y., Ph.D., Associate Professor, Department of Marine Science and Technology, Faculty of Fisheries and Marine Science, IPB University, Kampus IPB Dramaga, Bogor 16680, Indonesia.
- Email: *naulita@ipb.ac.id*
- ORCID: 0000-0002-4931-3783
- Web of Science ResearcherID: ABF-9349-2021
- Scopus Author ID: 54781750900
- Homepage: https://itk.ipb.ac.id/~itkipb/dr-ir-yuli-naulita-m-si/

HOW TO CITE THIS ARTICLE

Koropitan, A.F.; Khaldun, M.H.I.; Naulita, Y., (2022). Impact of tropical cyclone Marcus on ocean subsurface and surface layers. Global J. Environ. Sci. Manage., 8(3): 353-368.

DOI: 10.22034/gjesm.2022.03.05

url: https://www.gjesm.net/article_248202.html